



Scroll heat sink: A novel heat sink with the moving fins inserted between the cooling fins

Tae Young Kim, Dong-Kwon Kim, Sung Jin Kim *

School of Mechanical, Aerospace and System Engineering, Korea Advanced Institute of Science and Technology, Daejeon 305-701, Republic of Korea

ARTICLE INFO

Article history:

Received 15 November 2007

Received in revised form 21 March 2008

Available online 5 May 2008

ABSTRACT

In this paper, a new type of a fan-integrated heat sink named a scroll heat sink is proposed and demonstrated. The most striking feature of the scroll heat sink is that heat dissipation and fluid pumping occurs simultaneously in the whole cooling space without requiring any additional space for a fan module. In the scroll heat sink, the moving fins, which rotate with two eccentric shafts, are inserted between the fixed (cooling) fins. By a relative motion between the moving fins and the cooling fins, a coolant is drawn into the space between them, takes heat away from the cooling fins, and the heated coolant is discharged out of the heat sink. In the present study, an experimental investigation is performed in order to demonstrate the concept of the scroll heat sink. Average coolant velocities and thermal resistances of the scroll heat sink are measured for various rotating speeds of the moving fins from 200 rpm to 500 rpm. Experimental results show that measured flow rates of the coolant are almost linearly proportional to the rotating speed of the moving fins. A theoretical model is also developed to estimate the required pumping power and the thermal resistance, and validated using experimental results. The theoretical model shows that optimized scroll heat sinks have lower thermal resistances than optimized plate-fin heat sinks under the fixed pumping power condition.

© 2008 Elsevier Ltd. All rights reserved.

1. Introduction

Recent advances in semiconductor technology have led to a significant increase in power densities encountered in electronic modules or devices [1,2]. As the power dissipation from the electronic devices increases, effective cooling technology becomes essential for reliable operation of electronic components [3,4]. For this reason, various types of cooling systems have been developed as thermal solutions. The fan-integrated heat sink is the most widely used type of the cooling device due to its high price-performance ratio. The fan-integrated heat sink is mainly comprised of the two parts, the fan module for pumping the coolant and the heat sink for enlarging the heat transfer area. Accordingly, a wide body of research has been conducted not only on heat sinks but also on cooling fans.

Many investigators have studied heat sinks using a number of approaches [5–7] in efforts to improve their thermal performance. Various types of heat sinks with distinctive shapes have been suggested in addition to the conventional plate-fin and pin-fin heat sinks [8–11]. Investigations of working conditions, such as tip clearance [12] and direction of the coolant flow, on the thermal performance of heat sinks have been carried out. The performance of cooling fans has also been the subject of much attention because

the thermal performance of the heat sink depends on the velocity of the coolant passing through fins of the heat sink [13,14].

As noted above, considerable efforts have been aimed at making fan-integrated heat sinks more efficient by improving the performance of each component, the fan module and the heat sink. However, fan-integrated heat sinks currently being used in the field do not effectively use the total cooling space. For all existing fan-integrated heat sinks, the volumes for the heat sink and the fan are separated and are regarded as inviolable spaces with respect to each other. The spaces for the heat sink and the fan module are only designated for dissipating heat and for pumping coolant, respectively. If the entire space reserved for the cooling system were used simultaneously both for coolant pumping and for heat transfer, the heat sink size could be increased from that of fan-integrated heat sink in the same cooling space. This idea led to the conceptualization of a novel cooling system, namely, the scroll heat sink [15]. In the scroll heat sink, instead of the fan blades, the moving fins are inserted between the cooling fins and pump the coolant, as in the scroll compressor. The coolant flow is generated by the relative motion between the moving fins and the cooling fins. Coolant pumping and heat dissipation occurs simultaneously in the whole cooling space, as the cooling fins play a double role of coolant pumping and heat dissipation.

The aim of the present study is to propose and demonstrate a new concept for fan-integrated heat sinks, named the scroll heat sink, for which coolant pumping and heat transfer are combined

* Corresponding author. Tel.: +82 42 869 3043; fax: +82 42 869 8207.
E-mail address: sungjinkim@kaist.ac.kr (S.J. Kim).

Nomenclature

A	area, m^2	y	cartesian coordinate
d	distance between centers of two circles, m	<i>Greek symbols</i>	
D_h	hydraulic diameter, $m \equiv \frac{4A}{P}$	ε	porosity
e	eccentricity of the eccentric shafts, $m \equiv \frac{Hpe}{H+pe/2}$	μ	viscosity of the coolant
H	height of the heat sink, m	θ	thermal resistance, K/W
k	thermal conductivity, W/m K	ρ	density of the coolant
L	length of the heat sink, m	<i>Subscripts</i>	
p	pitch between adjacent fixed (or cooling) fins, m	bm	bulk mean
Pr	Prandtl number	fin	fin
r	radius of the small circle, m	in	inlet of the heat sink
R	radius of the large circle, m	max	maximum
Re	Reynolds number $\equiv \frac{\rho U D_h}{\mu}$	opt	optimum value
t	maximum fin thickness, m; time, s	scroll	scroll heat sink
T	temperature, K	w	wall
U	average coolant velocity, m/s		
W	width of the heat sink, m		

in order to make better use of the total cooling space. In the scroll heat sink, the moving fins are placed between the cooling fins and rotate with eccentric shafts. By the relative motion between the moving fins and the cooling fins, the coolant is drawn into the space between them, takes heat away from the cooling fins, and the heated coolant is discharged out of the heat sink. In the present study, the concept of the scroll heat sink is demonstrated through an experimental investigation. Average coolant velocities and thermal resistances of the scroll heat sink were measured for various rotating speeds of the moving fins. From the experimental results, we found that the average coolant velocity generated by the relative motion of fins proportionally increases with increasing rotational speed of the moving fins. A theoretical model is also developed to estimate the required pumping power and the thermal resistance, and validated using experimental results. The thermal performance of the scroll heat sink is optimized with the theoretical model and compared to that of the optimized plate-fin heat sink.

2. Working principle and design method

The schematic diagrams of the scroll heat sink are presented in Fig. 1. The scroll heat sink features two sets of fins, moving and cooling (fixed) fins, as shown in Fig. 1b. The moving fins and the cooling fins are connected to a moving substrate and a fixed substrate, respectively. The fixed substrate and the cooling fins are positioned on top of an electronic component and used for dissipating heat from the electronic component to the coolant. Two eccentric shafts are integrated with a coupler link and rotate with the same phase by an electrical motor. The moving fins rotate with the eccentric shafts because the moving substrate and the moving fins are connected to the coupler link.

The basic pumping mechanism of the scroll heat sink is similar to that of scroll compressors [16]. As the name implies, the shape of fins of the scroll heat sink is also modeled after the shape of blades of the scroll compressor. Fig. 2 depicts cross-sectional views of the cooling fins and the moving fins. These figures show how the relative motion between the moving fins and the cooling fins can generate the coolant flow in one direction. While the moving fins rotate, the moving fins and the cooling fins come into contact at a certain orbit angle (120° , Fig. 2c) and out of contact at another orbit angle (240° , Fig. 2e). During this period (120° – 240°), the moving fins keep in contact with the cooling fins, and the trapped fluid is squeezed out of the heat sink due to the relative motion between the moving fins and the cooling fins. As the coolant is discharged,

the volume of the gaps between the cooling fins and the moving fins increases and the pressure between them decreases. In this period, 240° – 300° of the orbit angle, cold coolant is drawn into the gaps and is heated until it is discharged out of the heat sink.

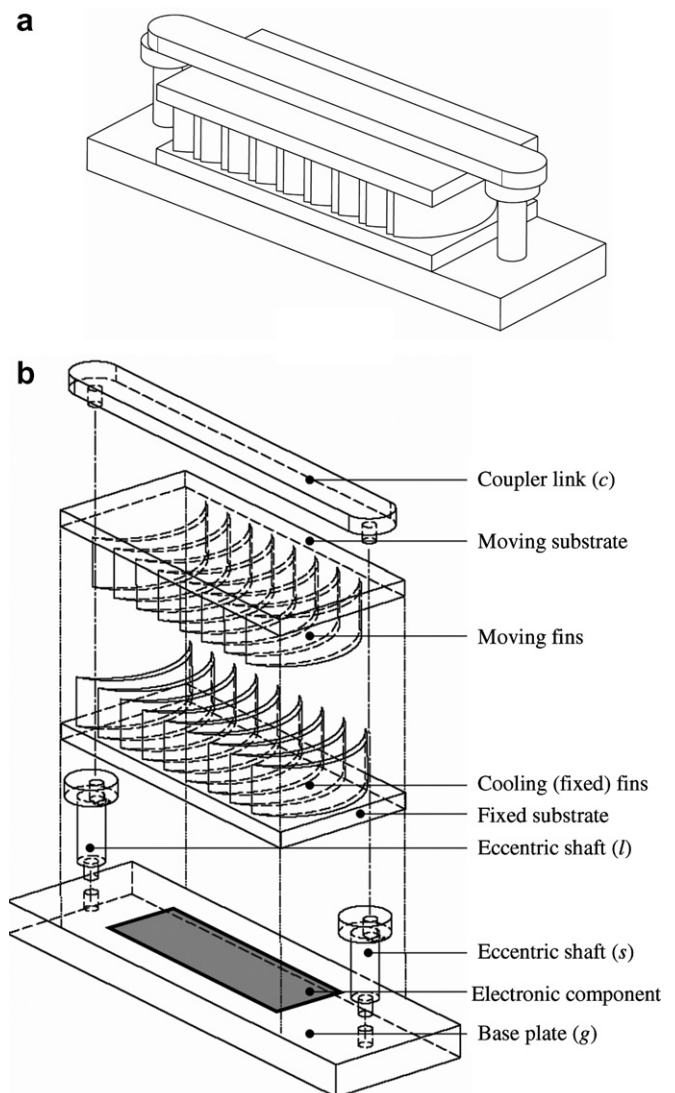


Fig. 1. Schematic diagrams of the scroll heat sink: (a) after assembling all the parts and (b) exploded schematic diagram.

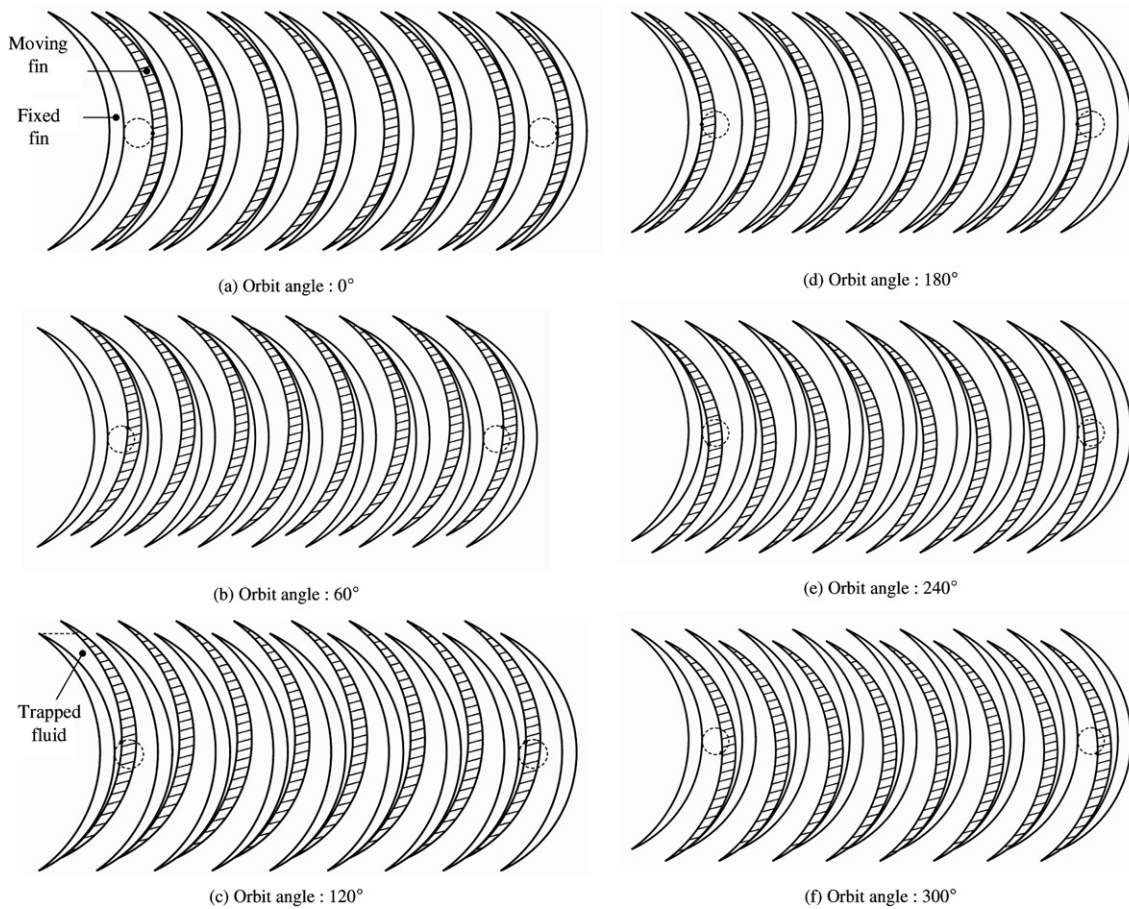


Fig. 2. Working principle of the scroll heat sink.

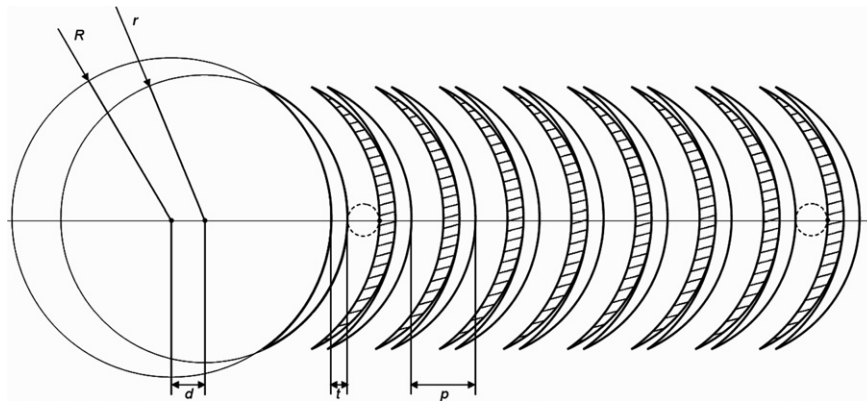


Fig. 3. Dimensions of the scroll heat sink.

There are two periods that the moving fins and the cooling fins are not in contact during one revolution (60° – 120° , 240° – 300°). There are another two periods that the moving fins and the cooling fins are in a point contact during one revolution (120° – 240° , 300° – 60°). These two types of periods occur by turns. Therefore, a series of intake and discharge of the coolant occur twice each in one cycle. In this manner, pumping of the coolant and dissipation of heat occurs simultaneously in the scroll heat sink.

The shape of fins is one of the main factors influencing the pumping and cooling efficiencies in the present system. As mentioned above, the shape of fins of the scroll heat sink resembles a part of a scroll of the scroll compressor in order to increase the pumping efficiency of the scroll heat sink. The dimensions of fins

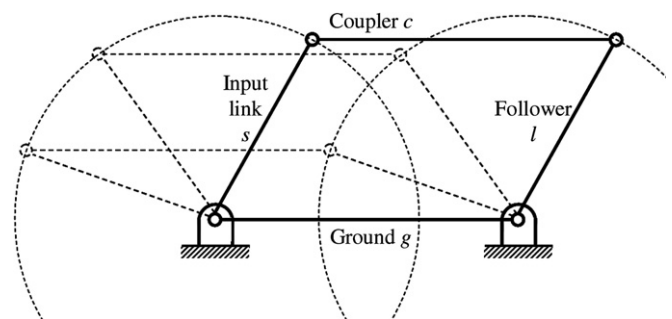


Fig. 4. Parallelogram linkage.

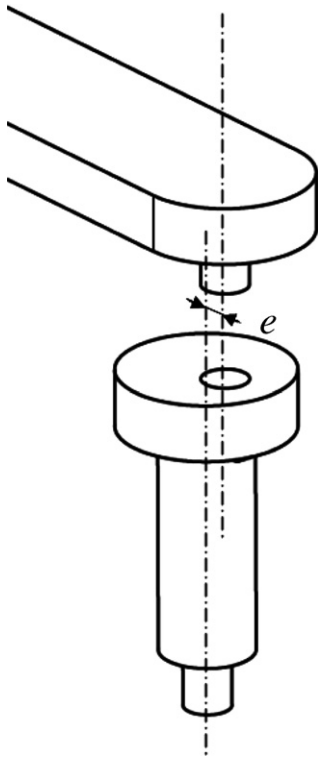


Fig. 5. Schematic diagram of the coupler link and the eccentric shaft.

for the scroll heat sink are presented in Fig. 3. As shown in this figure, the shapes of the cooling fins and the moving fins are identical. The shape of fins is defined by two circles whose centers are spaced d apart. The following geometrical relationships should be satisfied:

$$d = t + R - r \quad (1)$$

$$p = 2(t + R - r) \quad (2)$$

The working principle of the parallelogram linkage is applied to the moving parts of the scroll heat sink in order to make the moving fins rotate between the cooling fins. As shown in Fig. 4, the lengths of the input link s and the follower link l are identical in the parallelogram four-bar linkage. The orientation of the coupler link c does not change while it rotates. In the scroll heat sink, one eccentric shaft shown in Fig. 5 is used as the input link s and the other shaft is used as the follower link l . The eccentricity e , the length of the input link s and the follower link l , should satisfy the following relationship in order to avoid interference between the moving fins and the cooling fins during rotation

$$e = R - r \quad (3)$$

3. Experimental apparatus and procedure

In the previous section, the working principle and the design method of the scroll heat sink were described. It is in order to present experimental apparatus and procedure for demonstrating the proposed concept. Fig. 6a shows the moving fins and the cooling fins that are precisely fabricated using a CNC machine. The dimen-

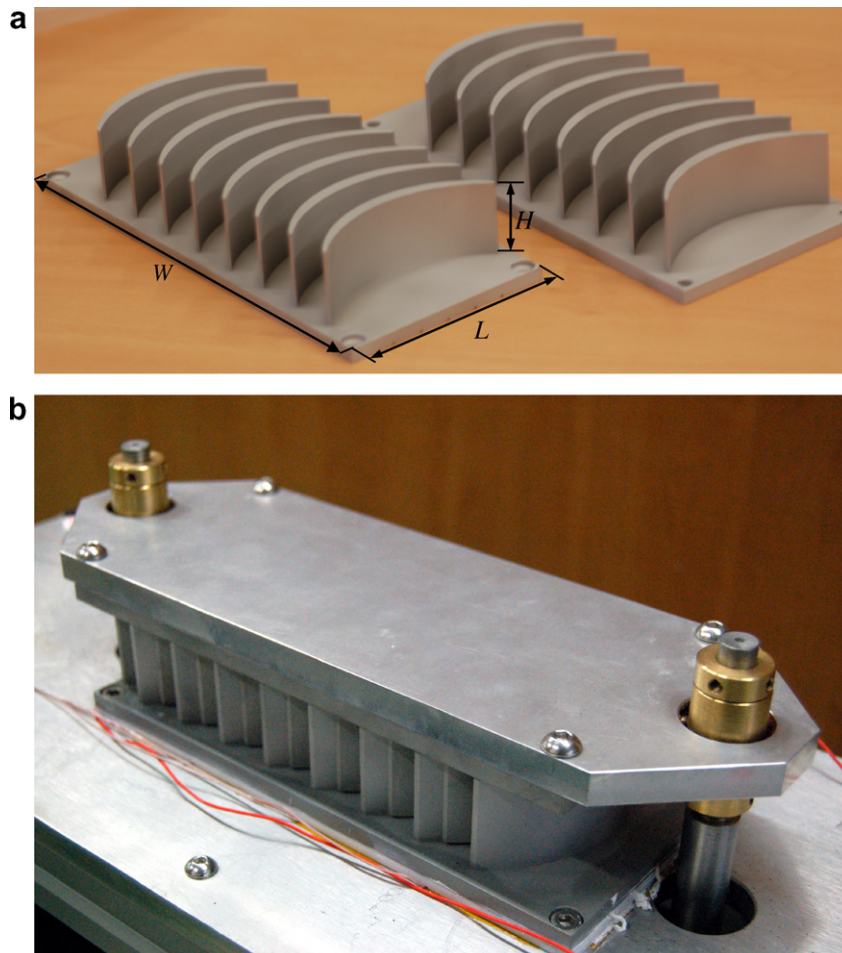


Fig. 6. Photographs of the scroll heat sink: (a) the cooling fins and the moving fins and (b) after assembling the moving fins and the cooling fins.

sions of fins are shown in Table 1. These fins are made of aluminum alloy 6063 ($k = 171 \text{ W/m K}$) and no additional surface treatment is applied.

Fig. 6b shows a photo of the scroll heat sink after assembling the moving and the cooling fins. The heater is attached to the bottom surface of the fixed substrate, and the thermal grease is applied between the heater and the substrate in order to reduce the contact resistance. The heater is fabricated using Kapton coated stainless steel with $0.25 \mu\text{m}$ thickness and is connected to a DC power supply. To reduce heat loss, the bottom surface of the heater is placed on a 3 mm thick Teflon[®] ($k = 0.2 \text{ W/m K}$) insulation block. Ten thermocouples are attached to the fixed substrate and the Teflon block for measuring the maximum base temperature of the scroll heat sink and the heat loss through the insulation layer.

The whole system for driving the scroll heat sink is shown in Fig. 7. An electric motor is connected to the gear box which is linked to an eccentric shaft and makes the shaft rotate. A timing belt under the base plate facilitates same phase rotation of the two eccentric shafts. The rotating speed of the moving fins and the moving substrate connected to the eccentric shafts is controlled by a motor controller. From the point of view of the total cooling space, the scroll heat sink has the advantage of not requir-

ing the additional space for the fan module, even though it still requires the space for an electric motor. In the present study, the moving fins and the moving substrate are made of aluminum 6063, which is chosen due mainly to economical and easy fabrication. For this reason, the electrical motor is somewhat large because it has to have enough power to rotate the heavy moving part of the assembly, as shown in Fig. 7. However, the size of the electrical motor could be significantly reduced by manufacturing the moving parts with a light material such as an acrylic. In this case its size would be equivalent to that of a conventional motor.

Table 1

Dimensions of the scroll heat sink (m)

Length of the heat sink, L	0.08
Height of the heat sink, H	0.03
Width of the heat sink, W	0.14
Maximum fin thickness, t	0.005
Radius of the large circle, R	0.055
Radius of the small circle, r	0.05

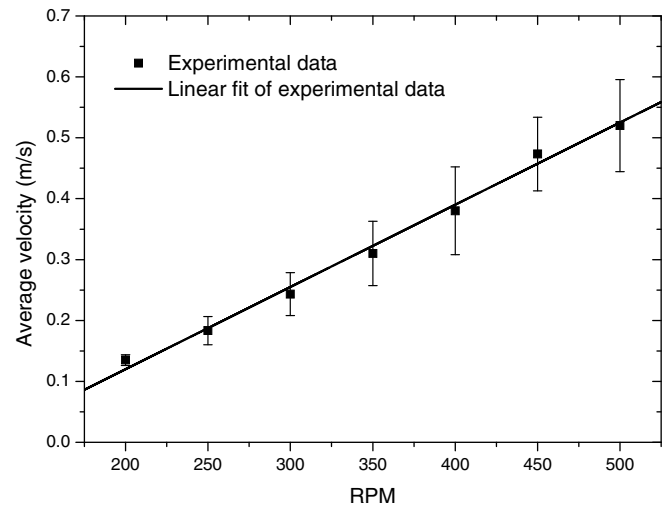


Fig. 8. Average coolant velocities as a function of the RPM of the moving fins.

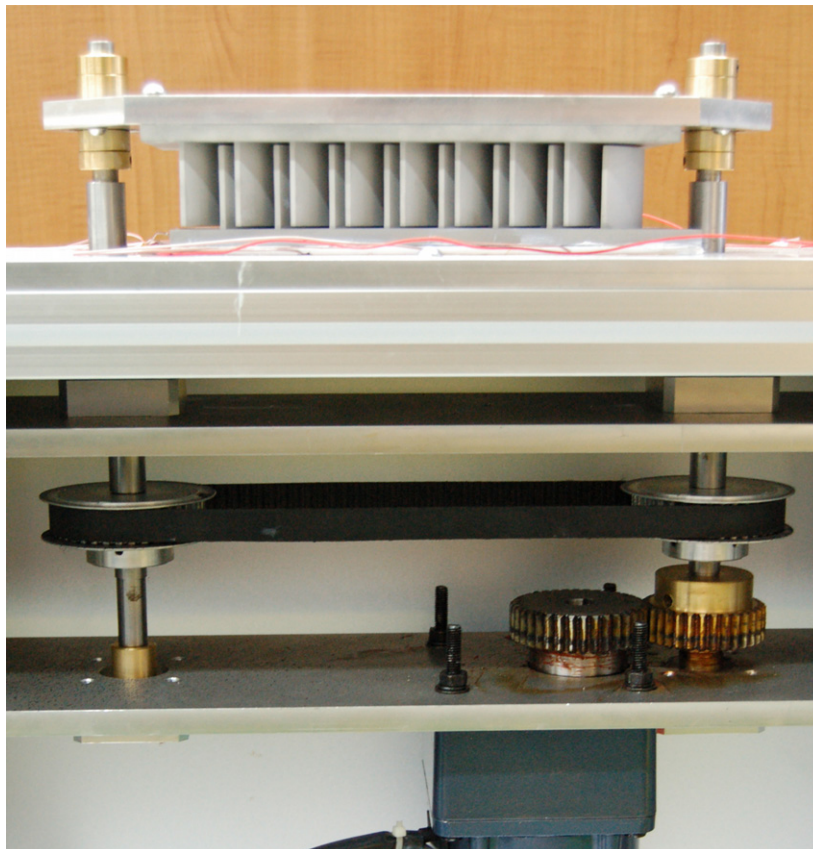


Fig. 7. Whole system for driving the scroll heat sink.

The test procedures were as follows: The rotating speed of the moving fins is varied from 200 rpm to 500 rpm with an increment of 50 rpm. The desired RPM of the moving substrate is set by the motor controller and the heater is powered up to a heat load of 80 W and allowed to be stabilized. The heat load is calculated by measuring the voltage drop and the current through the heater.

The steady-state was assumed when the temperature difference between the maximum base temperature of the scroll heat sink and the ambient temperature is maintained less than 0.1 °C during 2 min. The temperatures are therein measured by acquiring signals from the thermocouples with a NI PXI. The time and area averaged air velocities at the outlet of the heat sink are measured using a hot wire anemometer.

From the acquired experimental results, we could obtain the thermal performance of the scroll heat sink in terms of the thermal resistance, which is defined by

$$\theta = (T_{w,max} - T_{bm,in})/q \tag{4}$$

The actual heat flow rate q is calculated by subtracting the heat loss from the total heat rate supplied by the power supply.

4. Results and discussion

Average coolant velocities generated by the relative motion between the moving fins and the cooling fins are obtained from the experimental investigation and shown in Fig. 8. It is shown that average coolant velocity is almost linearly proportional to the RPM of the moving fins. This is because the coolant flow rate generated in the scroll heat sink is given by multiplying the RPM of the moving fins with the volume of the trapped fluid between the moving fins and the cooling fins. The cut-off frequency at which the coolant flow is not generated in spite of the rotary motion of the moving fins is observed to be in the vicinity of 75 rpm. The experimental

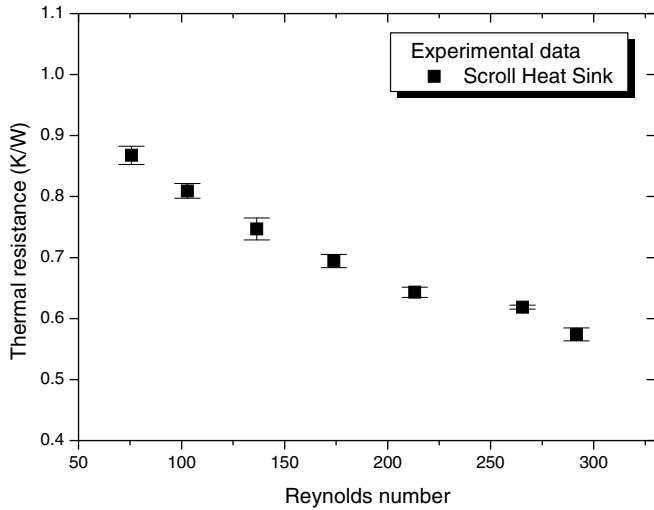


Fig. 9. Experimental results for thermal resistances of the scroll heat sink.

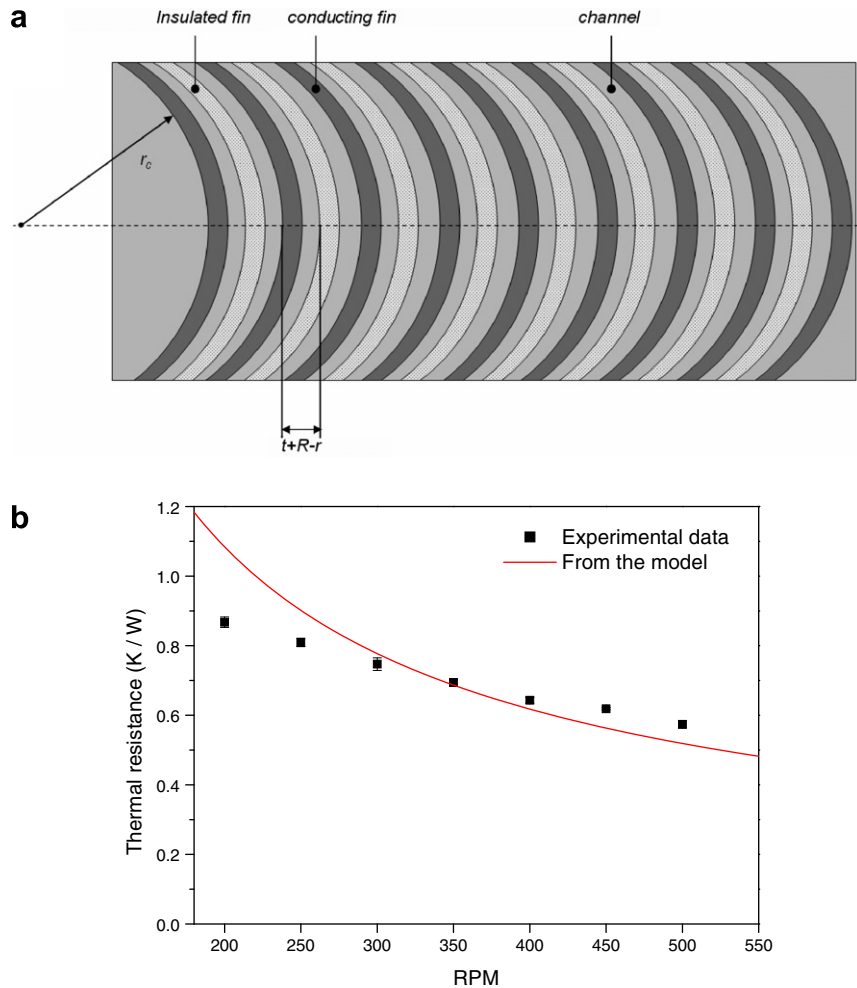


Fig. 10. Model for predicting the thermal performance of the scroll heat sink: (a) cross-sectional view of the equivalent heat sink and (b) predicted thermal resistances.

results for thermal resistances of the scroll heat sink are shown in Fig. 9. The thermal resistance of the scroll heat sink decreases as the rotating speed increases. This is because the thermal resistance of the heat sink decrease with increasing coolant flow rate.

We have also developed a model for predicting the pumping power and the thermal resistance of the scroll heat sink. According to the model, the thermal resistance of scroll heat sink is simply given as

$$\theta = \frac{1}{h(\eta A_{\text{fin}} + A_{\text{base}})} + \frac{1}{\rho c_f Q} \quad (5)$$

The details for determining the coefficients and parameters, appearing in Eq. (5), are presented in Appendix A. The thermal resistances predicted from the model are presented in Fig. 10. The thermal resistances obtained from the model are in good agreement with the experimental results. Therefore, the present model is suitable for predicting the thermal performance of the scroll heat sink. By using the model, thermal resistances of the optimized scroll and plate-fin heat sinks under the fixed pumping power condition are compared. The constraint of the fixed pumping power physically means that the power required to drive the coolant through the heat sinks is fixed. By comparing thermal resistances of the optimized plate-fin and scroll heat sinks, a contour map is presented in Fig. 11. Fig. 11 depicts the logarithm of the ratio of thermal resistances of the optimized plate-fin and scroll heat sinks ($\log(\theta_{\text{opt,plate}}/\theta_{\text{opt,scroll}})$) as a function of dimensionless pumping power and length. In Fig. 11, in the region where the logarithm of the ratio is positive, the thermal resistance of the optimized scroll heat sink is smaller than that of the optimized plate-fin heat sink. On the other hand, the thermal resistance of the optimized plate-fin heat sink is smaller than that of the optimized scroll heat sink when the logarithm of the ratio is negative. The contour map indicates that optimized scroll heat sinks have lower thermal resistances than optimized plate-fin heat sinks in practical situations. It is worth mentioning that the additional volume required to place the fan module is not taken into account when the thermal resistances of the plate-fin and the scroll heat sinks are compared. As mentioned before, the scroll heat sink does not require additional space for the fan blades because the moving fins for pumping the coolant are already integrated in the heat sink. Therefore, Fig. 11 means the thermal performance of the scroll heat sink is better even though the size of the cooling system is smaller.

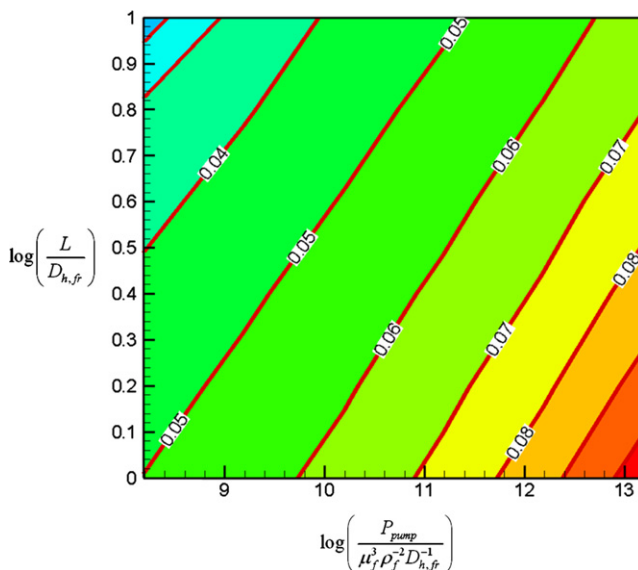


Fig. 11. Comparison of the thermal resistances of the optimized heat sinks in terms of dimensionless length and pumping power ($k_s/k_f = 6.4 \times 10^3$, $Pr = 0.707$).

It is to be noted that the scroll heat sink is superior to the equivalent plate-fin heat sink in the thermal performance because of its high heat transfer coefficient. In the case of the plate-fin heat sink, the boundary layer becomes thicker at the fin surface along the flow direction. Thus, the heat transfer coefficient becomes smaller along this direction. On the other hand, in the case of the scroll heat sink, the growth of the boundary layers is hindered by the relative motion between the moving fins and the cooling fins. Therefore, the relative motion between the moving fins and the cooling fins makes it possible for the scroll heat sink to have the higher thermal performance than the equivalent plate-fin heat sink in the smaller cooling space.

5. Conclusion

In this paper, the scroll heat sink is suggested and demonstrated as a means of efficiently utilizing the cooling space and enhancing the thermal performance of the heat sink for electronics cooling applications. The most remarkable feature of the scroll heat sink is that heat dissipation and fluid pumping occurs simultaneously in the given space without requiring any additional space for a fan module. In the scroll heat sink, the moving fins, which rotate with the eccentric shafts, are placed between cooling (fixed) fins. By the relative motion between the moving fins and the cooling fins, a coolant is drawn into the space between them, takes heat away from the cooling fins, and is discharged out of the heat sink. The coolant flow generated by the relative motion between fins moves through the heat sink in one direction. Experiments were performed in order to demonstrate the proposed concept of the scroll heat sink. In the experiments, the rotating speed of the moving fins varies from 200 rpm to 500 rpm. Experimental results show that the generated coolant flow rate in the scroll heat sink is proportional to the rotating speed of the moving fins. A theoretical model is also developed to estimate the required pumping power and the thermal resistance, and validated using experimental results. The theoretical model shows that optimized scroll heat sinks have lower thermal resistances than optimized plate-fin heat sinks under the fixed pumping power condition. The relative motion between the moving fins and the cooling fins enhances the thermal performance of the scroll heat sink by periodically disturbing the boundary layer development at cooling fin surfaces. Due to its high thermal performance, the scroll heat sink is expected to be suitable for a next generation cooling solution.

Acknowledgements

This work was supported by the Korea Science and Engineering Foundation (KOSEF) through the National Research Lab. Program funded by the Ministry of Science and Technology (No. M1060000022406J000022410).

Appendix A. Analysis of fluid flow and heat transfer in the scroll heat sink

In this section, we explain how the required pumping power and the thermal resistance for the scroll heat sink can be calculated.

If we try to calculate the velocity and temperature fields accurately in order to obtain the pumping power and the thermal resistance, modeling can be cumbersome due to the complex topology of the heat sinks and the transient nature of the problem. Because our main interest lies in the macroscopic quantities, it is wise to model the complex structure as a simple one which has the same macroscopic properties and time-averaged quantities. Therefore, in the present study, the scroll heat sink is modeled as an equivalent heat sink with curved fins which has the same porosity, fin surface

area, and fin number. The cross-sectional view for the equivalent heat sink is shown in Fig. 10a. The porosity ε , the hydraulic diameter D_h , the aspect ratio α , and the radius of the curvature of the channel of the equivalent heat sink r_c are given as

$$\varepsilon = 1 - \left(\int_{-0.5L}^{0.5L} (R+t-r+(r^2-y^2)^{0.5} - (R^2-y^2)^{0.5}) dy \right) / (L(t+R-r)) \quad (\text{A.1})$$

$$D_h = 2H(t+R-r)\varepsilon / (H + (t+R-r)\varepsilon) \quad (\text{A.2})$$

$$\alpha = H / ((t+R-r)\varepsilon) \quad (\text{A.3})$$

$$r_c \sin^{-1}(0.5L/r_c) = 0.5R \sin^{-1}(0.5L/R) + 0.5r \sin^{-1}(0.5L/r) \quad (\text{A.4})$$

The pressure drop between the inlet and the outlet is given as

$$\Delta p = C_2 \gamma_{\Delta p} f_{fd} Re_{D_h} L_{eff} U / D_h^2 \quad (\text{A.5})$$

where the friction factor ratio between the curved pipe and the straight pipe $\gamma_{\Delta p}$, the friction factor for the steady fully-developed flow in the straight rectangular channel f_{fd} , the effective channel length L_{eff} , the mean velocity U , the Reynolds number Re_{D_h} , and the Dean number K are given from

$$\gamma_{\Delta p} = 0.108K^{0.5} \quad (\text{A.6})$$

$$f_{fd} Re_{D_h} = 4.70 + 19.64(1 + (\text{MAX}[\alpha, \alpha^{-1}])^{-2}) / (1 + (\text{MAX}[\alpha, \alpha^{-1}])^{-1})^2 \quad (\text{A.7})$$

$$L_{eff} = 2r_c \sin^{-1}(0.5L/r_c) \quad (\text{A.8})$$

$$U = Q / (WH\varepsilon) \quad (\text{A.9})$$

$$Re_{D_h} = \rho U D_h / \mu \quad (\text{A.10})$$

$$K = Re_{D_h} (0.5D_h/r_c)^{0.5} \quad (\text{A.11})$$

Eqs. (A.6) and (A.7) are obtained from Refs. [17,18], respectively. The thermal performance of the scroll heat sink can be evaluated by the thermal resistance. The thermal resistance of the scroll heat sink is simply given as Eq. (5), where c_f and Q are specific heat and volume flow rate of the coolant, respectively. The heat transfer coefficient h , the fin efficiency η , the total fin area A_{fin} , the total base area A_{base} , and the Nusselt number for the steady fully-developed flow in the straight rectangular channel Nu_{fd} are determined from

$$h = C_3 \gamma_h Nu_{fd} k_f / D_h \quad (\text{A.12})$$

$$\eta = \tanh(mH) / (mH) \quad (\text{A.13})$$

$$A_{fin} = H(R \sin^{-1}(0.5L/R) + r \sin^{-1}(0.5L/r))W / (t+R-r) \quad (\text{A.14})$$

$$A_{base} = WL\varepsilon \quad (\text{A.15})$$

$$Nu_{fd} = 4.502 - 7.945/\text{MAX}[\alpha, \alpha^{-1}] + 12.30/\text{MAX}[\alpha, \alpha^{-1}]^2 - 9.489/\text{MAX}[\alpha, \alpha^{-1}]^3 + 2.912/\text{MAX}[\alpha, \alpha^{-1}]^4 \quad (\text{A.16})$$

$$m = \sqrt{\frac{h(2R \sin^{-1}(0.5L/R) + 2r \sin^{-1}(0.5L/r))}{k_s L(t+R-r)(1-\varepsilon)}} \quad (\text{A.17})$$

where γ_h is the Nusselt number ratio between the curved pipe and the straight pipe, C_2 and C_3 are the empirical coefficients for the friction factor ratio and the heat transfer coefficient ratio between the real flow and the steady-state flow, respectively. γ_h , C_2 and C_3 can be obtained from Refs. [17,19,20], respectively.

References

- [1] S. Oktay, R.J. Hannemann, A. Bar-Cohen, High heat from a small package, *Mech. Eng.* 108 (3) (1986) 36–42.
- [2] A. Bar-Cohen, Thermal management of electric components with dielectric liquids, in: J.R. Lloyd, Y. Kurosaki (Eds.), *Proceedings of ASME/JSME Thermal Engineering Joint Conference*, vol. 2, 1996, pp. 15–39.
- [3] F.P. Incropera, Convection heat transfer in electronic equipment cooling, *J. Heat Transfer* 110 (1988) 1097–1111.
- [4] W. Nakayama, Thermal management of electronic equipment: a review of technology and research topics, *Appl. Mech. Rev.* 39 (12) (1986) 1847–1868.
- [5] M.B. Dogruoz, M. Urdaneta, A. Ortega, Experiments and modeling of the hydraulic resistance and heat transfer of in-line square pin fin heat sinks with top by-pass flow, *Int. J. Heat Mass Transfer* 48 (2005) 5058–5071.
- [6] D. Kim, S.J. Kim, Forced convection in microstructures for electronic equipment cooling, *J. Heat Transfer* 121 (1999) 639–645.
- [7] T. Liou, S. Chen, K. Shih, Numerical simulation of turbulent flow field and heat transfer in a two-dimensional channel with periodic slit ribs, *Int. J. Heat Mass Transfer* 45 (2002) 4493–4505.
- [8] J.L. Xu, Y.H. Gan, D.C. Zhang, X.H. Li, Microscale heat transfer enhancement using thermal boundary layer redeveloping concept, *Int. J. Heat Mass Transfer* 48 (2005) 1662–1674.
- [9] K. Tatsumi, K. Noda, K. Nakabe, The effect of cut-fin array arrangement on heat transfer and friction characteristics, in: *Proceedings the 6th KSME-JSME Thermal and Fluids Engineering Conference*, No. tfec6-470, 2005.
- [10] S. Garimella, C. Sobhan, Transport in microchannels – a critical review, *Ann. Rev. Heat Transfer* 13 (2003) 1–50.
- [11] D.B. Tuckerman, R.F.W. Pease, High-performance heat sinking for VLSI, *IEEE Electron Device Lett.* 2 (1981) 126–129.
- [12] J.M. Min, S.P. Jang, S.J. Kim, Effective of tip clearance on the cooling performance of a microchannel heat sink, *Int. J. Heat Mass Transfer* 47 (2004) 1099–1103.
- [13] X. Tian, Cooling fan reliability: failure criteria, accelerated life testing, modeling and qualification, in: *Reliability and Maintainability Symposium*, 2006, pp. 380–385.
- [14] M. Strum, Fan Reliability Guide, HP Internal Project Report, 2004.
- [15] S.J. Kim, D.K. Kim, T.Y. Kim, Korean Patent No. 10-0743268, Taiwanese Patent No. 96129477, PCT No. PCT/KR2007/003761, 2007.
- [16] Y. Chen, N.P. Halm, E.A. Groll, J.E. Braun, Mathematical modeling of scroll compressors – Part I: compression process modeling, *Int. J. Refrig.* 25 (2002) 731–750.
- [17] Y. Mori, W. Nakayama, Study on forced convective heat transfer in curved pipes, *Int. J. Heat Mass Transfer* 8 (1965) 67–82.
- [18] R.K. Shah, A.L. London, *Laminar Flow Forced Convection in Ducts*, Academic Press, 1978.
- [19] R. Siegel, M. Perlmutter, Heat transfer for pulsating laminar duct flow, *ASME J. Heat Transfer* 84 (1962) 111–123.
- [20] A. Bouhadji, N. Djilali, Forcing of unsteady separated flow and convective heat transfer via bulk upstream oscillations, *Int. J. Heat Fluid Flow* 24 (2003) 77–90.